The Astrophysical Journal Letters, 788:L14 (5pp), 2014 June 10 doi:10.1088/2041-8205/788/1/L14

SN 2008D: A WOLF–RAYET EXPLOSION THROUGH A THICK WIND

Gilad Svirski and Ehud Nakar
Raymond and Beverly Sackler School of Physics and Astronomy, Tel Aviv University, Tel Aviv 69978, Israel
Received 2014 March 13; accepted 2014 May 9; published 2014 May 27

ABSTRACT

Supernova (SN) 2008D/XRT 080109 is considered to be the only direct detection of a shock breakout from a regular SN to date. While a breakout interpretation was favored by several papers, inconsistencies remain between the observations and current SN shock breakout theory. Most notably, the duration of the luminous X-ray pulse is considerably longer than expected for a spherical breakout through the surface of a type Ibc SN progenitor, and the X-ray radiation features, mainly its flat spectrum and its luminosity evolution, are enigmatic. We apply a recently developed theoretical model for the observed radiation from a Wolf–Rayet SN exploding through a thick wind and show that it naturally explains all of the observed features of SN 2008D X-ray emission, including the energetics, the spectrum, and the detailed luminosity evolution. We find that the inferred progenitor and SN parameters are typical for an exploding Wolf–Rayet. A comparison of the wind density found at the breakout radius and the density at much larger radii, as inferred by late radio observations, suggests an enhanced mass-loss rate taking effect about 10 days prior to the SN explosion. This finding joins accumulating evidence for a possible late phase in the stellar evolution of massive stars, involving vigorous mass loss a short time before the SN explosion.

Key words: radiation mechanisms: non-thermal – stars: mass-loss – stars: Wolf–Rayet – supernovae: general – supernovae: individual (2008D) – X-rays: bursts

Online-only material: color figure

1. INTRODUCTION

The X-ray transient XRT 080109, associated with supernova (SN) 2008D, was discovered by *Swift*/XRT (Soderberg et al. 2008). Later observations in optical/UV led to its classification as a type Ibc SN, favoring a Wolf–Rayet (WR) progenitor (Soderberg et al. 2008; Mazzali et al. 2008; Malesani et al. 2009; Modjaz et al. 2009). The X-ray signal of SN 2008D is the most convincing candidate for a shock breakout of a standard SN. Unlike other observed X-ray SN birth signals, which are all of rare broad-lined Ic SNe associated with gamma-ray bursts (e.g., SN2006aj/GRB060218; Campana et al. 2006), the serendipitous discovery and the spectroscopic classification of SN 2008D suggest that it was a common signal, produced by a common Ibc SN (Soderberg et al. 2008).

Nevertheless, the detailed X-ray observations are still unexplained. The initial rise time, the following light curve, and the spectrum are different than the ones predicted for a standard SN breakout, namely a spherical breakout from the stellar surface (e.g., Chevalier & Fransson 2008; Katz et al. 2010; Nakar & Sari 2010; Sapir et al. 2011). In order to explain the prolonged rise time, Soderberg et al. (2008) suggested a breakout through a thick wind. Balberg & Loeb (2011) modeled the luminosity and the duration of the breakout pulse through a wind and found that it can explain SN 2008D. The rise time was alternatively explained as a result of an aspherical breakout (Couch et al. 2011). However, due to the lack of detailed theoretical models for the spectrum and the luminosity evolution under the two scenarios,[1] neither could be confronted with the detailed observed spectrum and light curve. As often occurs in the absence of a consensual explanation, a burst of a mildly relativistic jet was also suggested (Xu et al. 2008; Li 2008; Mazzali et al. 2008), though this model has no predictions in terms of the expected X-ray emission that can be compared to the observations.

[1] A major progress in modeling aspherical breakouts was only recently achieved by Matzner et al. (2013).

We recently developed a detailed theoretical model for the emission from an SN breakout through a thick wind (Svirski & Nakar 2014). Here, based on this model, we show that a scenario in which a WR explodes through a thick wind naturally solves all inconsistencies and provides, without a need to invoke a significant breakout asphericity or an unconventional explosion scenario, an optimal explanation for the X-ray observations of SN 2008D.

In Section 2, we describe the observations and indicate their tension with a standard SN breakout interpretation. We then summarize, in Section 3, our model for WR SNe exploding through a thick wind (Svirski et al. 2012; Svirski & Nakar 2014) and show, in Section 4, that this scenario explains the X-ray observations. We discuss the mass-loss history in Section 5 and conclude in Section 6.

2. OBSERVATIONS VERSUS STELLAR SURFACE BREAKOUT

2.1. Observations

Several groups analyzed the *Swift* and *Chandra* X-ray data (Soderberg et al. 2008; Li 2008; Mazzali et al. 2008; Xu et al. 2008; Modjaz et al. 2009), with results that are generally in good agreement across the groups. The analysis by Modjaz et al. (2009) is the most comprehensive and, unless otherwise stated, the numbers we quote refer to this work.

The rise time of the X-ray transient is 50 ± 30 s according to Modjaz et al. (2009) and $\sim$100 s according to Soderberg et al. (2008); therefore, we take the rise time to be $\approx$80 s, which is consistent with both. The X-ray luminosity peaks at $3.8 \pm 1 \times 10^{43}$ erg s^{-1} and Modjaz et al. (2009) fits its evolution to a broken power law in time: the luminosity at $60 < t < 300$ s ($t = 0$ is the onset of the X-ray emission) is best described by a decaying power law, $L_X \propto t^{\alpha}$, with $\alpha = -0.8 \pm 0.2$, whereas the luminosity at $t > 300$ drops sharply, $\alpha = -3.4 \pm 0.6$. The total estimated energy output in X-ray is $\sim 10^{46}$ erg (Soderberg et al. 2008; Chevalier & Fransson 2008; Modjaz et al. 2009).

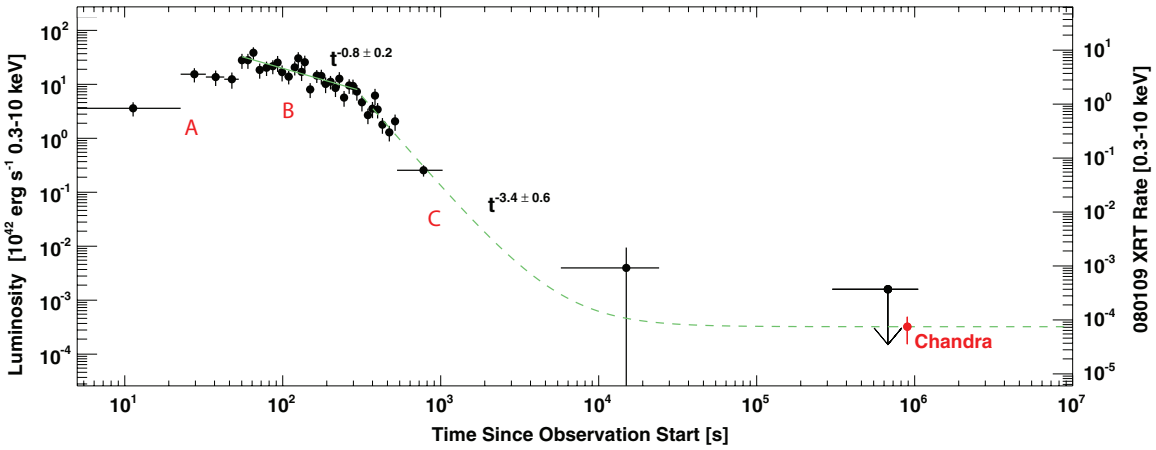

Figure 1. X-ray luminosity evolution, adapted with permission from Modjaz et al. (2009). Black dots are *Swift*/XRT data and the red dot is a *Chandra* measurement. This light curve is expected, according to the model of Svirski & Nakar (2014), where (A) is the rising breakout pulse, (B) is the collisionless shock fast cooling phase, accompanied by a flat X-ray spectrum, and (C) is the slow cooling phase, with a fast decay of the X-ray signal.

(A color version of this figure is available in the online journal.)

A *Chandra* observation at day 10 reads $3.2 \pm 1.7 \times 10^{38}$ erg s^{-1}, indicating that the steep $t > 300$ s decay is halted around 10^4 s or changes trend prior to the *Chandra* observation. Figure 1 sketches the X-ray luminosity evolution during the first 10 days, based on Figure 1 from Modjaz et al. (2009).

All groups carried out a spectral fit of the X-ray radiation to a power-law model, $N(E) \propto E^{-\Gamma}$, integrating over the transient duration (520 s in Modjaz et al. 2009 and slightly shorter elsewhere). We quote here the results of these power-law fits and skip additional fits that involved a blackbody model, because a blackbody radiation is not expected according to our breakout interpretation. The spectrum is best fit by a single power law with a photon spectral index $\Gamma = 2.3 \pm 0.3$ (Soderberg et al. 2008; Li 2008; Xu et al. 2008; Mazzali et al. 2008) or $\Gamma = 2.1^{+0.3}_{-0.4}$ (Modjaz et al. 2009). All power-law fits are consistent with a flat spectrum, $\nu F_\nu = $ Const, or slightly softer, i.e., a comparable amount of energy in each photon logarithmic frequency scale across the frequency range of *Swift*, 0.3–10 keV. Soderberg et al. (2008) also reported a significant softening of the X-ray spectrum between the peak and the emission 400 s later, during the rapid decay phase.

Later observations, at frequencies softer than X-rays, correspond to a standard Ibc SN (e.g., Soderberg et al. 2008; Modjaz et al. 2009), and we only quote here the radio observations that are relevant for our analysis in Section 4. Soderberg et al. (2008) analyzed Very Large Array observations, identified synchrotron emission, and inferred a shock radius, $\approx 3 \times 10^{15}$ cm at $t \approx 5$ days, implying a mean shock velocity, $v \approx 0.25c$ (c is the speed of light) over the first 5 days. In addition, they found that the observations indicate a standard wind density profile.

2.2. A Standard Breakout?

In a standard breakout scenario, namely a spherical shock breakout through a stellar surface, the duration of the initial pulse is dominated by the light crossing time across the progenitor (e.g., Klein & Chevalier 1978). A WR radius is expected to reach up to a few times 10^{11} cm, implying a light crossing time of $\sim$10 s, in contrast with the observed $\sim$300 s of $L_X \geqslant 10^{43}$ erg s^{-1}. We note that the progenitor radius is under debate, ranging (based on UV/optical observations) from 10^{11} cm (Soderberg et al. 2008; Rabinak & Waxman 2011) to 10^{12} cm (Chevalier & Fransson 2008), but even the latter estimate matches a light crossing time that is an order of magnitude below the observed duration.

One could argue that the moderate $\alpha = -0.8 \pm 0.2$ initial luminosity decay, lasting until $t \approx 300$ s, is marginally consistent with the $\alpha = -4/3$ expected during the planar phase of a standard breakout (Piro et al. 2010; Nakar & Sari 2010, hereafter NS10). However, a planar time, $R_*/v \sim 300$ s, implies a stellar radius, $R_* \sim 4 \times 10^{12}$ cm, for $v = 0.25c$ (Soderberg et al. 2008). R_* and v correspond to a breakout energy of $\sim 10^{47}$ erg, an order of magnitude above the observed, and a UV signal that is too bright (Chevalier & Fransson 2008). While uncertainty in the rise time and the breakout velocity may reduce this tension, it cannot completely remove it. In addition, such a radius is not expected for a WR progenitor, as implied by the Ibc classification.

Regarding the spectrum, the observed radiation from a WR SN breakout is expected to deviate significantly from thermal equilibrium (Katz et al. 2010; NS10), and therefore a blackbody spectrum is not expected. Instead, we expect a radiation that peaks at a few keV, likely within the *Swift*/XRT 0.3–10 keV detection window (e.g., NS10; Sapir et al. 2011), but is fainter elsewhere. NS10 predict a $\nu F_\nu \propto \nu^\beta$ with $0.5 < \beta < 1$ up to the peak and an exponential decay above it. However, when fitted to a power-law spectrum, the observations are consistent with a flat or slightly negative spectrum across the complete *Swift* detection range.

3. THE EMISSION FROM A WOLF–RAYET SUPERNOVA EXPLODING THROUGH A THICK WIND

SN ejecta that expand into a surrounding wind give rise to an interaction layer, composed of a forward shocked wind and a reverse shocked ejecta. Assuming a spherical shock, an outer (pre-explosion) stellar envelope density profile with a polytropic index of three, and a standard wind density profile, $\rho_w \propto r^{-2}$, the radius and velocity of the interaction layer evolve as $r \propto t^{0.875}$ and $v \propto t^{-0.125}$, respectively (Chevalier 1982; Svirski et al. 2012). The optical depth of the unshocked wind ahead of the shock evolves as $\tau \propto r^{-1}$, or approximately $\tau \propto t^{-1}$.

In Svirski & Nakar (2014), we derive a model for the radiation from a WR SN exploding through a thick wind, and we quote

the relevant findings below. If the optical depth of the wind surrounding the star is $>c/v$, where c is the speed of light and v is the SN shock speed, then the radiation mediated shock that crosses the star envelope continues into the wind and breaks out when the optical depth of the unshocked wind decreases to $\tau \approx c/v$. The bolometric luminosity while $\tau > 1$ is

$$L(t) \approx 3.5 \times 10^{43}\, t_{\rm bo,m}\, v_{\rm bo,10}^{3} \left(\frac{t}{t_{\rm bo}}\right)^{-0.4} \ {\rm erg\,s^{-1}}, \qquad (1)$$

where $v_{\rm bo}$ is the shock velocity at the time of breakout, $v_{\rm bo,10} = v_{\rm bo}/10^{10}\,{\rm cm\,s^{-1}}$, $t_{\rm bo}$ is the breakout time and $t_{\rm bo,m} = t_{\rm bo}/{\rm minute}$. Observationally, $t_{\rm bo}$ is also roughly the rise time of the breakout pulse.

The shock velocity at the breakout depends on the explosion energy, E, the SN ejecta mass, $M_{\rm ej}$, and the breakout time:

$$v_{\rm bo} \approx 6 \times 10^{9}\, M_5^{-0.31} E_{51}^{0.44} t_{\rm bo,m}^{-0.25}\ {\rm cm\,s^{-1}}, \qquad (2)$$

where $E_{51} = E/10^{51}$ erg and $M_5 = M_{\rm ej}/5\,M_\odot$.

The breakout pulse of a fast shock exploding through a thick wind was first discussed by Balberg & Loeb (2011). This pulse has a non-thermal spectrum that peaks at a few keV. Unlike a standard breakout, the rise time is $\sim(R_{\rm bo}/v_{\rm bo})$ (where $R_{\rm bo}$ is the breakout radius) rather than $\sim(R_*/c)$, and the shock breakout has no planar phase. Following the breakout, a collisionless shock replaces the radiation-mediated shock and a layer of hot shocked electrons, with a temperature $T_h \geqslant 60\,{\rm keV}$ (hereafter, a temperature, T, denotes an energy, k_BT, where k_B is the Boltzmann constant), forms behind the shock (Katz et al. 2011; Murase et al. 2011). The efficient cooling of these hot electrons dominates the SN luminosity, and is sustained by inverse Compton over soft photons that were deposited by the radiation-mediated shock that crossed the star. This soft radiation injects into the interaction region a fraction, $f_{\rm inj} \approx (1/5)(R_*/R_{\rm bo})$, of the luminosity powered by the interaction, at a characteristic temperature, $T_{\rm inj}$. The condition

$$\frac{T_{\rm inj}}{m_e c^2/\tau^2} \ll f_{\rm inj} \ll 1, \qquad (3)$$

where m_e is the electron mass, implies a flat or nearly flat spectrum, $\nu F_\nu \approx$ Const across the range $T_{\rm inj} \lesssim T \lesssim \min(m_e c^2/\tau^2, T_h)$. This condition is typically satisfied for WR stars exploding through a thick wind.

At $\tau \ll 1$, the emission takes the form of a standard core–collapse SN, with no wind. The interaction signal is fainter and dominated by single scattering of soft photons by the hot shocked layer. However, a small fraction of the soft photons goes through multiple scattering and produces an X-ray signal. Since at this stage $T_h \sim 200$ keV, each collision upscatters a photon by an average factor of $\sim$4, and it takes $n = \ln(T_X/T_{\rm SN})/\ln(4)$ collisions to bring a soft $T_{\rm SN}$ photon to an X-ray temperature, T_X. A signature of such an X-ray signal is a decay pattern, $L_X(t) \propto t^{-n}$, and a continuous softening of the X-ray spectrum.

4. A COHERENT PICTURE OF SN 2008D

Our model predicts the X-ray luminosity evolution and the spectrum observed from an SN exploding through a thick WR wind. Assuming such a scenario, the luminosity evolution depends on $t_{\rm bo}$, which is directly observed, and $v_{\rm bo}$, which can be inferred from the observations in multiple independent ways. The spectrum at $\tau \gtrsim 1$ depends on $f_{\rm inj}$ and $T_{\rm inj}$, both inferred from theoretical considerations. Below, we show that our model predictions, despite being over-constrained by the observations, are all satisfied.

The most robust constraint on the shock breakout velocity comes from the observed luminosity peak, the value of which is highly sensitive to the velocity but far less so to the breakout time, and rather insensitive to the time since breakout (see Equation (1)). Substituting $t_{\rm bo} = 80$ s and $L_{\rm bo} = 3.8 \pm 1 \times 10^{43}\,{\rm erg\,s^{-1}}$ (Modjaz et al. 2009) in Equation (1) yields $0.84 < v_{\rm bo,10} < 1$. Balberg & Loeb (2011) obtained a similar estimate using the observed $E_{\rm bo} \sim L_{\rm bo} t_{\rm bo}$ and $t_{\rm bo}$. An independent alternative estimate of $v_{\rm bo}$ comes from the optical depth at breakout. Following the breakout, due to fast cooling, the X-ray luminosity decays slowly as the shock traverses the range $1 < \tau < \tau_{\rm bo}$. As $\tau \propto t^{-1}$, the ratio between the time of transition to a sharp luminosity drop and the rise time indicates the breakout optical depth, $\tau_{\rm bo} \approx (300/80) \approx 4$, implying $v_{\rm bo,10} \approx 0.8$, in good agreement with the first estimate. Yet, a third independent estimate is obtained from Equation (2). Combining a progenitor mass, $5\,M_\odot \lesssim M \lesssim 7\,M_\odot$, and an explosion energy, $2 \lesssim E_{51} \lesssim 6$, (Soderberg et al. 2008; Mazzali et al. 2008) with $t_{\rm bo} = 80$ s implies $0.75 \lesssim v_{\rm bo,10} \lesssim 1.3$, providing a second sanity check. Combining these three estimates and accounting for the uncertainty in the rise time, the peak luminosity, and the exact τ of transition to a slow cooling, we infer a breakout velocity in the range of $0.6 \lesssim v_{\rm bo,10} \lesssim 1.2$.

Next, we examine the observed spectrum of the X-ray transient. The X-ray radiation is dominated by the cooling of the collisionless shock that forms after the breakout and its spectrum is determined by $f_{\rm inj}$ and $T_{\rm inj}$. We estimate $T_{\rm inj}$ to be the characteristic SN radiation temperature calculated in NS10 Equation (41). The published range of the progenitor mass and explosion energy, along with an assumed WR radius, $R_* = 5\,R_\odot = 3.5 \times 10^{11}$ cm, imply an initial $T_{\rm inj} \sim 300\,{\rm eV}$ at $t = 80\,{\rm s}$, dropping sharply to $T_{\rm inj} \sim 30\,{\rm eV}$ at $t = 300\,{\rm s}$. A simple estimate, $v_{\rm bo} t_{\rm bo}$, implies a breakout radius, $R_{\rm bo} \approx 6 \times 10^{11}$ cm, and a respective $f_{\rm inj} \sim 0.1$ for $R_* = 5\,R_\odot$. These $f_{\rm inj}$ and $T_{\rm inj}$ values satisfy Equation (3) and imply, at $80 \lesssim t \lesssim 300\,{\rm s}$, a flat spectrum that initially spans across the range $0.3 \lesssim T \lesssim 50\,{\rm keV}$, and later widens to $0.03 \lesssim T \lesssim 100\,{\rm keV}$. This is consistent with the flat spectrum observed by *Swift*/XRT within its detection window of 0.3–10 keV. Note that while a radius smaller than $5\,R_\odot$ by a factor of a few implies somewhat lower $f_{\rm inj}$ and initial $T_{\rm inj}$, these still yield a rather flat spectral slope. Hence, an approximately flat spectrum is a robust prediction of our model and it is unaffected by the freedom, in the progenitor mass and radius and in the explosion energy, implied by the current range of these values presented in the literature.

The flat X-ray spectrum also explains the first phase of the X-ray luminosity evolution. Inverse Compton provides a fast cooling of the shock as long as $\tau \gtrsim 1$, and therefore one would expect Equation (1) to apply for $80 \lesssim t \lesssim 300\,{\rm s}$. However, the observations indicate that over this period, $L_X \propto t^\alpha$, with an index $\alpha = -0.8 \pm 0.2$, only marginally consistent with the predicted $\alpha = -0.4$ implied by Equation (1). In fact, this difference is expected. While most of the initial X-ray spectrum is covered by the *Swift*/XRT window, by $t = 4t_{\rm bo}$ about half of the spectral logarithmic range falls outside of the *Swift*/XRT window, implying an X-ray decay that is slightly faster than that predicted for the bolometric luminosity, as observed.

At $\tau < 1$ ($t > 300\,{\rm s}$), the shock becomes slow cooling and the soft SN radiation soon becomes the dominant component

of the bolometric luminosity. At this stage, an X-ray signal decaying as t^{-n} is expected. An initial photon temperature of a few eV, matching the first few hours after the explosion, implies that three subsequent Compton scatters are required to upscatter a photon to within the *Swift*/XRT detection window. Therefore, the X-ray luminosity observed by *Swift*/XRT should follow $L_X \propto \tau^3 \propto t^{-3}$, in agreement with the observed X-ray luminosity at $t > 300$ s (after a few hours, n, should rise to four, still consistent with the observed slope). Here, τ is the optical depth of the hot layer, which is comparable, due to the slow cooling, to the optical depth of the unshocked wind. The X-ray signal at this stage is expected to soften, as indeed reported by Soderberg et al. (2008).

The X-ray luminosity measured by *Chandra* at day 10 is higher than expected by the t^{-3} trend described above. This may be accounted for by inverse Compton upscattering of optical photons to X-ray by relativistic electrons (accelerated by the collisionless shock). Soderberg et al. (2008) reported observation of synchrotron emission, an imprint of relativistic electrons, and estimates of their induced X-ray luminosity (Soderberg et al. 2008; Chevalier & Fransson 2008) agree with the *Chandra* observation.

5. MASS-LOSS HISTORY

Applying our model to SN 2008D suggests an increased mass-loss rate during the days that preceded the explosion. Soderberg et al. (2008) used the radio observations at day 5, with the common microphysical values $\epsilon_e \approx \epsilon_B \approx 0.1$ (Chevalier & Fransson 2006, ϵ_e and ϵ_B are the fractions of the shock energy carried by relativistic electrons and magnetic field, respectively), to infer $A_* \approx 1$, typical for Galactic WR stars (e.g., Cappa et al. 2004), where $A_* = A/(5 \times 10^{11}\,\mathrm{g\,cm^{-1}})$ and $\rho = Ar^{-2} = \dot{M}/4\pi r^2 v_w$. In contrast, our breakout conditions imply $A_* \approx 20$, above the typical WR range, shortly before the explosion.

Balberg & Loeb (2011), who first raised this tension, suggested that it reflects either a pre-explosion increase of A_* or an ϵ_B lower than the 0.1 assumed by Soderberg et al. (2008). However, based on Chevalier & Fransson (2006), a combination of the luminosities in both radio and X-rays, and the accumulated shock kinetic energy, unambiguously determine ϵ_e, ϵ_B, and A_*. Combining the radio observations with the observed X-ray luminosity at day 10 imposes $\epsilon_B \approx \epsilon_e$, and demanding $A_* \approx 20$ implies $\epsilon_B \approx \epsilon_e \approx 5 \times 10^{-3}$, requiring a shock energy of $\sim 10^{49}$ erg. A calculation of the kinetic energy accumulated as the shock traverses an $A_* \approx 20$ wind from breakout to day five yields an energy lower by an order of magnitude, while the combination of $A_* \approx 1$ and $\epsilon_B \approx \epsilon_e \approx 0.1$ better fits the implied shock energy, making the lower ϵ_B scenario less plausible. A pre-explosion increased A_* is further indicated by the 5 day average shock velocity $\approx 0.25c$ (Soderberg et al. 2008), which implies, for a $v \propto t^{-0.125}$ deceleration through 3×10^{15} cm, a breakout velocity, $v_{\rm bo} \approx 1.5 \times 10^{10}\,\mathrm{cm\,s^{-1}}$, above our inferred range. This tension is relieved for a termination of the enhanced wind density at $\lesssim 10^{14}$ cm, which matches, for a typical WR wind velocity $v_w = 1000\,\mathrm{km\,s^{-1}}$, to a mass-loss enhancement ~ 10 days before the explosion.

6. CONCLUSION

We offer the first coherent picture of SN 2008D X-ray observations, including a first explanation for the observed flat X-ray spectrum across the *Swift*/XRT 0.3–10 keV window during the first few hundred seconds, and a first account of the complete X-ray luminosity evolution of SN 2008D/XRT 080109, from breakout to $t \sim 1$ day. We find that a typical WR progenitor and typical SN parameters offer the optimal explanation for the observations.

We apply our model for WR SNe exploding through a thick wind (Svirski & Nakar 2014) to the X-ray observations of SN 2008D. The model allows only little freedom in deriving physical parameters from the observations and it over-constrains the shock velocity. In addition, it enforces a flat X-ray spectrum at $\tau \gtrsim 1$ and a t^{-3} to t^{-4} X-ray luminosity decay at $\tau \ll 1$. Hence, the combination of an observed $t_{\rm bo}$ and an observationally inferred $v_{\rm bo}$ uniquely determine the X-ray luminosity and spectrum as a function of time. Despite these tight constraints, the observations satisfy all the predictions of the model. Accordingly, SN 2008D had a compact progenitor ($R_* \lesssim 3 \times 10^{11}$ cm), presumably a WR, that exploded through a thick wind of a standard wind density profile, $\rho \propto r^{-2}$, with $R_{\rm bo} \approx 6 \times 10^{11}$ cm, $v_{\rm bo} \approx 8 \times 10^9\,\mathrm{cm\,s^{-1}}$, $\tau_{\rm bo} \approx 4$ and $n_{\rm bo} \sim 10^{13}\,\mathrm{cm^{-3}}$.

Observations of SN 2008D suggest that the explosion of the core was aspherical (Maund et al. 2009; Gorosabel et al. 2010). According to a recent theoretical prediction, if such an explosion gives rise to a significant deviation from spherical symmetry of the shock at the breakout, it implies a breakout shock velocity that is lower than a spherical breakout velocity, over major parts of the shock front (Matzner et al. 2013). The good agreement between our spherical model predictions and the observations, and the fact that the breakout velocity we infer, as well as the one estimated by Soderberg et al. (2008), are both rather high, as expected for spherical WR shock breakouts, suggest that the asphericity level of the shock at the breakout was low and its effect on the X-ray emission, as well as the dynamics, was minor.

Interestingly, a comparison of the shock velocity and wind density that we find at $R \sim 10^{12}$ cm, to that inferred by radio observations at $R \sim 3 \times 10^{15}$ cm, suggests that the mass-loss rate of the progenitor has increased by more than an order of magnitude during the few days that preceded the SN explosion. A pre-explosion enhanced mass loss may be a common feature of massive stars. Ofek et al. (2013) reported a mass-loss event just a month before SN 2010mc, likely the explosion of a luminous blue variable progenitor, and suggested a causal connection between the pre-explosion mass-loss burst and the explosion. Based on a sample of 16 type IIn SNe, Ofek et al. (2014) inferred that at least half of the type IIn SNe experience a similar pre-explosion outburst. Gal-Yam et al. (2014) identified SN 2013cu as an explosion of a WR progenitor and found indications for an increased mass-loss rate starting a year before the explosion. Our results for SN 2008D join these accumulating indications and suggest that at least some WR progenitors experience an increased mass-loss rate during a short period prior to their explosion. The excess mass loss in this case is due to a higher continuous mass loss, rather than the pre-explosion bursts that may characterize many type IIn SNe. Put together, these findings may indicate a general phase of enhanced mass loss in the late stellar evolution of massive stars, e.g., by a process as suggested by Shiode & Quataert (2014).

We thank the referee for helpful comments that improved this manuscript. G.S. and E.N. were partially supported by an ISF grant (1277/13), an ERC starting grant (GRB-SN 279369), and the I-CORE Program of the Planning and Budgeting Committee and The Israel Science Foundation (1829/12).

REFERENCES

Balberg, S., & Loeb, A. 2011, MNRAS, 414, 1715
Campana, S., Mangano, V., Blustin, A. J., et al. 2006, Natur, 442, 1008
Cappa, C., Goss, W. M., & van der Hucht, K. A. 2004, AJ, 127, 2885
Chevalier, R. A. 1982, ApJ, 258, 790
Chevalier, R. A., & Fransson, C. 2006, ApJ, 651, 381
Chevalier, R. A., & Fransson, C. 2008, ApJL, 683, L135
Couch, S. M., Pooley, D., Wheeler, J. C., & Milosavljević, M. 2011, ApJ, 727, 104
Gal-Yam, A., Arcavi, I., Ofek, E. O., et al. 2014, Natur, in press
Gorosabel, J., de Ugarte Postigo, A., Castro-Tirado, A. J., et al. 2010, A&A, 522, A14
Katz, B., Budnik, R., & Waxman, E. 2010, ApJ, 716, 781
Katz, B., Sapir, N., & Waxman, E. 2011, arXiv:1106.1898
Klein, R. I., & Chevalier, R. A. 1978, ApJL, 223, L109
Li, L.-X. 2008, MNRAS, 388, 603
Malesani, D., Fynbo, J. P. U., Hjorth, J., et al. 2009, ApJL, 692, L84
Matzner, C. D., Levin, Y., & Ro, S. 2013, ApJ, 779, 60
Maund, J. R., Wheeler, J. C., Baade, D., et al. 2009, ApJ, 705, 1139
Mazzali, P. A., Valenti, S., Della Valle, M., et al. 2008, Sci, 321, 1185
Modjaz, M., Li, W., Butler, N., et al. 2009, ApJ, 702, 226
Murase, K., Thompson, T. A., Lacki, B. C., & Beacom, J. F. 2011, PhRvD, 84, 043003
Nakar, E., & Sari, R. 2010, ApJ, 725, 904
Ofek, E. O., Sullivan, M., Cenko, S. B., et al. 2013, Natur, 494, 65
Ofek, E. O., Sullivan, M., Shaviv, N. J., et al. 2014, ApJ, submitted (arXiv:1401.5468)
Piro, A. L., Chang, P., & Weinberg, N. N. 2010, ApJ, 708, 598
Rabinak, I., & Waxman, E. 2011, ApJ, 728, 63
Sapir, N., Katz, B., & Waxman, E. 2011, ApJ, 742, 36
Shiode, J. H., & Quataert, E. 2014, ApJ, 780, 96
Soderberg, A. M., Berger, E., Page, K. L., et al. 2008, Natur, 453, 469
Svirski, G., & Nakar, E. 2014, arXiv:1402.4477
Svirski, G., Nakar, E., & Sari, R. 2012, ApJ, 759, 108
Xu, D., Watson, D., Fynbo, J., et al. 2008, in The 37th COSPAR Scientific Assembly (Montreal: COSPAR), 3512